Tokyo Climate Center, Japan Meteorological Agency

TCC News

Autumn 2023

Table of Contents: TCC News No. 74

El Niño Outlook (November 2023 - May 2024)

Atmospheric and oceanic indicators suggest that El Niño conditions have persisted in the equatorial Pacific since boreal spring this year. It is likely that these conditions will continue through boreal spring next year (80%) (article based on the El Niño outlook issued on 10 November 2023).

1. El Niño/La Niña

In October 2023, the sea surface temperature (SST) for the NINO.3 region was above normal with a deviation of +2.2°C, which was the same as August and September. SSTs were above normal in and around central and eastern parts of the equatorial Pacific. (Figures 1-1 and 1-3 (a)). Subsurface temperatures were also above normal in and around the central and eastern equatorial Pacific (Figures 1-2 and 1-3 (b)). In the atmosphere, convective activity over the same area was above normal, and easterly winds in the lower troposphere (i.e., trade winds) over the central equatorial Pacific were weaker than normal. These oceanic and atmospheric conditions indicate that El Niño conditions had persisted in this area since boreal spring.

A warm subsurface water volume in central and eastern parts of the equatorial Pacific (Figure 1-2) has caused ongoing elevated SSTs in the NINO.3 region. JMA's seasonal ensemble prediction system forecasts that this volume in central and eastern parts will move eastward and the NINO.3 SST will be above normal during the prediction period (Figure 1-4). In conclusion, it is likely that El Niño conditions will continue through boreal spring next year (80%) (Figure 1-5).

(https://www.data.jma.go.jp/tcc/tcc/products/elnino/outlook.html)

2. Western Pacific and Indian Ocean

The area-averaged SST in the tropical western Pacific (NINO.WEST) region was near normal in October, and is

likely to be near or below normal in boreal spring.

The area-averaged SST in the tropical Indian Ocean (IOBW) region was near normal in October, and is likely to be above normal until boreal winter and above normal in boreal spring.

(ITO Akira, Tokyo Climate Center)

* The SST normal for the NINO.3 region (5°S – 5°N, 150°W – 90°W) is defined as a monthly average over the latest sliding 30-year period (1993-2022 for this year).

* The SST normals for the NINO.WEST region (Eq. – 15°N, 130°E – 150°E) and the IOBW region (20°S – 20°N, 40°E – 100°E) are defined as linear extrapolations with respect to the latest sliding 30-year period, in order to remove the effects of significant long-term warming trends observed in these regions.

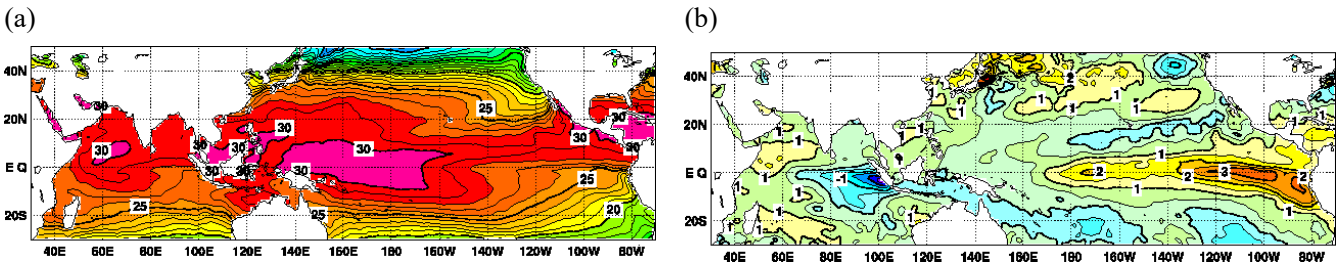

Figure 1-1 Monthly mean (a) sea surface temperatures (SSTs) and (b) SST anomalies in the Indian and Pacific Ocean areas for October 2023
The contour intervals are 1°C in (a) and 0.5°C in (b). The base period for the normal is 1991 – 2020.

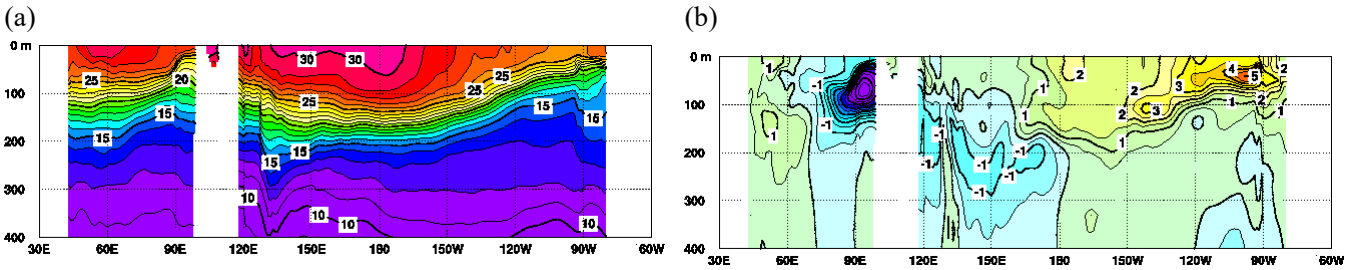

Figure 1-2 Monthly mean depth-longitude cross sections of (a) temperatures and (b) temperature anomalies in the equatorial Indian and Pacific Ocean areas for October 2023
The contour intervals are 1°C in (a) and 0.5°C in (b). The base period for the normal is 1991 – 2020.

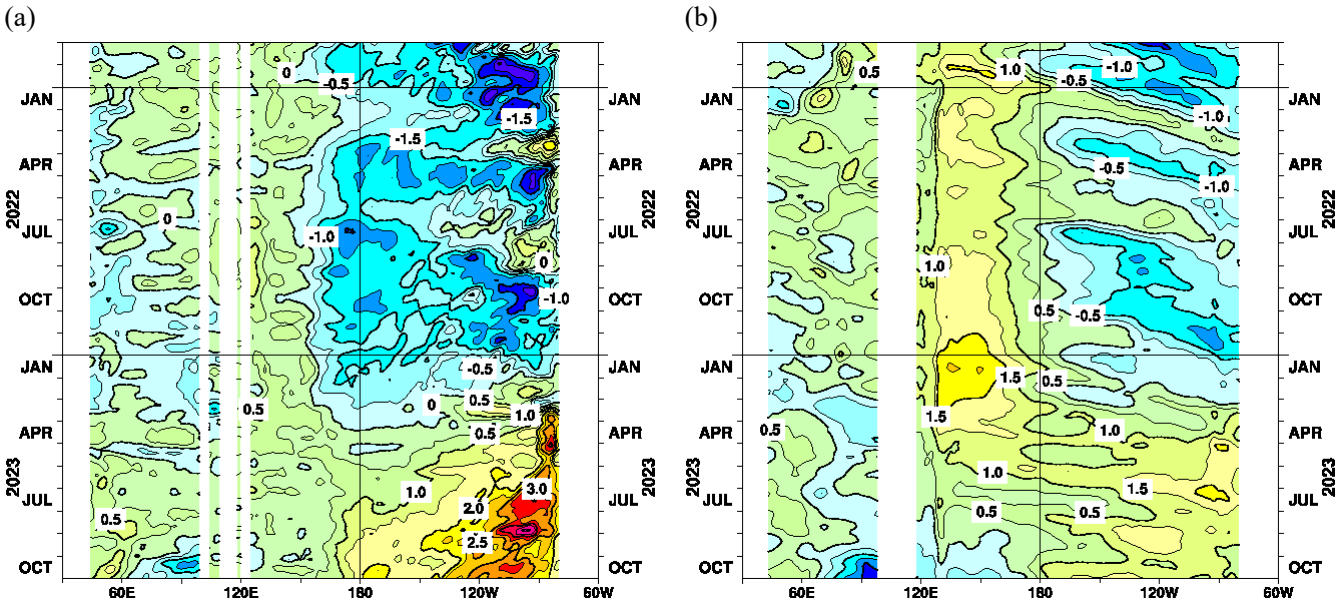

Figure 1-3 Time-longitude cross sections of (a) SST and (b) ocean heat content (OHC) anomalies along the equator in the Indian and Pacific Ocean areas

OHCs are defined here as vertically averaged temperatures in the top 300 m. The base period for the normal is 1991 – 2020.

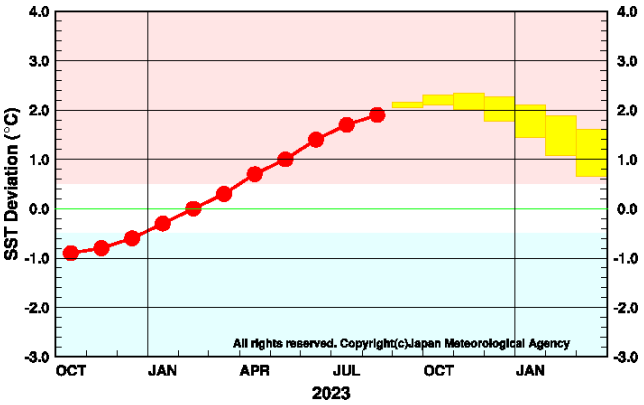

Figure 1-4 Outlook of NINO.3 SST deviation produced by the seasonal ensemble prediction system

This figure shows a time series of monthly NINO.3 SST deviations. The thick line with closed circles shows observed SST deviations, and the boxes show the values produced for up to six months ahead by the seasonal ensemble prediction system. Each box denotes the range into which the SST deviation is expected to fall with a probability of 70%.

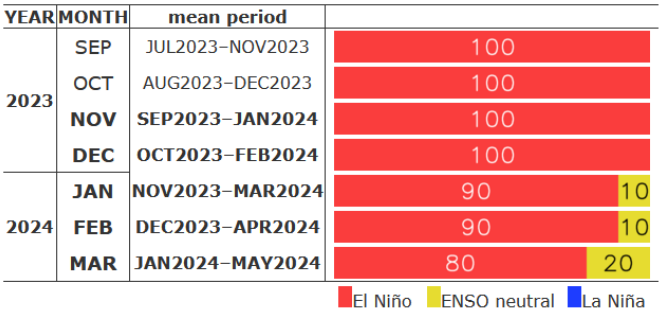

Figure 1-5 ENSO forecast probabilities based on the seasonal ensemble prediction system

Red, yellow and blue bars indicate probabilities that the five-month running mean of the NINO.3 SST deviation from the latest sliding 30-year mean will be +0.5°C or above (El Niño), between +0.4 and -0.4°C (ENSO-neutral) and -0.5°C or below (La Niña), respectively. Regular text indicates past months, and bold text indicates current and future months.

<<Table of contents <Top of this article

JMA's Seasonal Numerical Ensemble Prediction for Boreal Winter 2023/2024

This report outlines JMA's dynamical seasonal ensemble prediction for boreal winter 2023/2024 (December – February, referred to as DJF), which was used as a basis for JMA's operational three-month outlook issued on 21 November 2023. The outlook is based on the seasonal ensemble prediction system of the Coupled Atmosphere-ocean General Circulation Model (CGCM).

Summary: El Niño conditions have persisted in the equatorial Pacific since boreal spring this year, and are likely to

continue (80%) through boreal spring next year. In association, active convection is expected over central to eastern parts of the equatorial Pacific. Conversely, inactive convection is expected over eastern parts of the equatorial Indian Ocean to most of the Maritime Continent. In the lower troposphere, anti-cyclonic and cyclonic circulation anomalies straddling the equator are expected from the Indian Ocean to the Maritime Continent and the tropical Pacific, respectively, in association with tropical convection.

1. Sea surface temperatures

Figure 2-1 shows predicted SSTs (contours) and related anomalies (shading) for DJF. Positive anomalies are expected in central-to-eastern parts of the equatorial Pacific and in western parts of the Indian Ocean. Near-normal conditions are expected in eastern parts of the Indian Ocean and around the Maritime Continent. In conclusion, it is likely that El Niño conditions will continue (80%) through boreal spring next year.

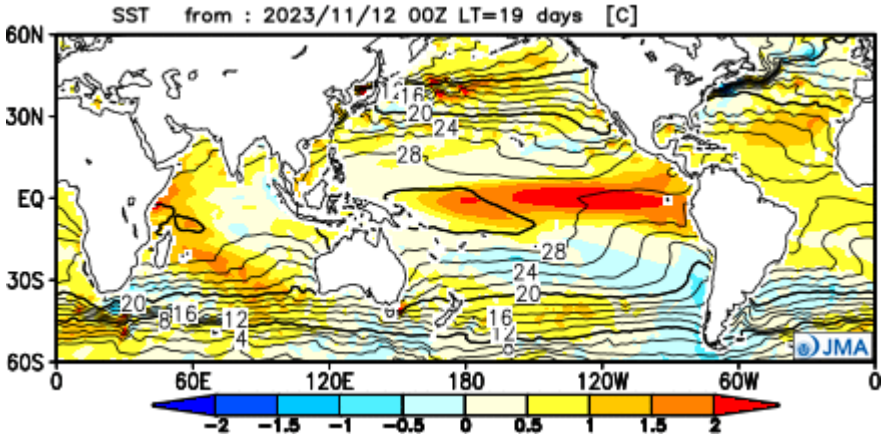

Figure 2-1 Predicted SSTs (contours) and SST anomalies (shading) for December–February 2023/2024 (ensemble mean of 51 members)

2. Prediction for the tropics and sub-tropics

Figure 2-2 (a) shows predicted precipitation (contours) and related anomalies (shading) for DJF. In association with ongoing El Niño conditions, precipitation is expected to be above normal over central-to-eastern parts of the equatorial Pacific and western parts of the equatorial Indian Ocean. Conversely, values are expected to be below normal over eastern parts of the equatorial Indian Ocean to most of the Maritime Continent.

Figure 2-2 (b) shows predicted velocity potential (contours) and related anomalies (shading) in the upper troposphere for DJF. In association with the precipitation anomalies described above, large-scale divergence anomalies are expected over the western Indian Ocean and the central tropical Pacific, and convergence anomalies are expected from the eastern Indian Ocean to the Maritime Continent.

Figure 2-2 (c) shows predicted stream functions (contours) and related anomalies (shading) in the upper troposphere for DJF. A stationary wave pattern with anti-cyclonic circulation anomalies near the Arabian Sea and cyclonic circulation anomalies over southern Eurasia are expected in association with anomalous convection over and around the Indian Ocean. Anti-cyclonic circulation anomalies straddling the equator are expected over the central-to-eastern tropical Pacific.

Figure 2-2 (d) shows predicted stream functions (contours) and related anomalies (shading) in the lower

troposphere for DJF. Anti-cyclonic and cyclonic circulation anomalies straddling the equator are expected from the Indian Ocean to the Maritime Continent and the tropical Pacific, respectively.

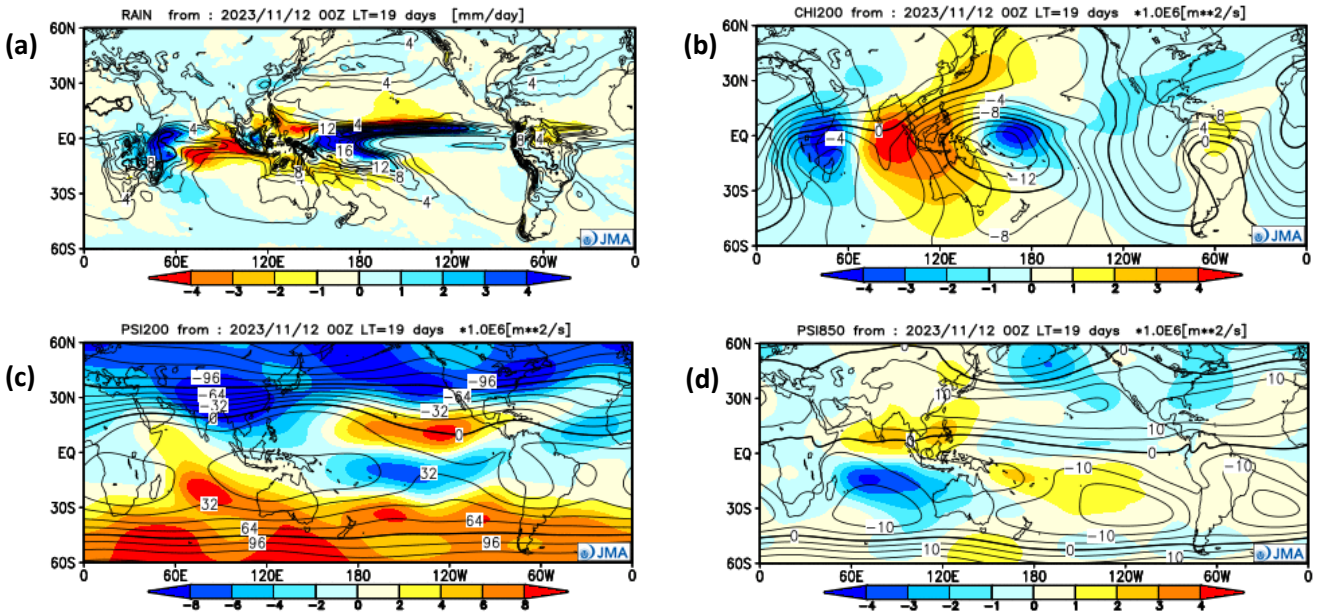

Figure 2-2 Predicted atmospheric fields over 60°N-60°S for December–February 2023/2024 (ensemble mean of 51 members)
(a) Precipitation (contours) and anomaly (shading). The contour interval is 2 mm/day. (b) Velocity potential at 200-hPa (contours) and anomaly (shading). The contour interval is 2 × 10^6 m^2/s. (c) Stream function at 200-hPa (contours) and anomaly (shading). The contour interval is 16 × 10^6 m^2/s. (d) Stream function at 850-hPa (contours) and anomaly (shading). The contour interval is 5 × 10^6 m^2/s.

3. Prediction for mid/high latitudes of the Northern Hemisphere

Figure 2-3 (a) shows predicted 500-hPa geopotential heights (contours) and related anomalies (shading) for DJF. Positive anomalies are expected over a wide area of East Asia and areas near Central Siberia, and negative anomalies are expected near the Aleutian Islands.

Figure 2-3 (b) shows predicted sea level pressure (contours) and related anomalies (shading) for DJF. The Aleutian Low is expected to be intensified over its normal position. Positive anomalies are expected over the eastern part of East Asia, corresponding to positive height anomalies at 500 hPa.

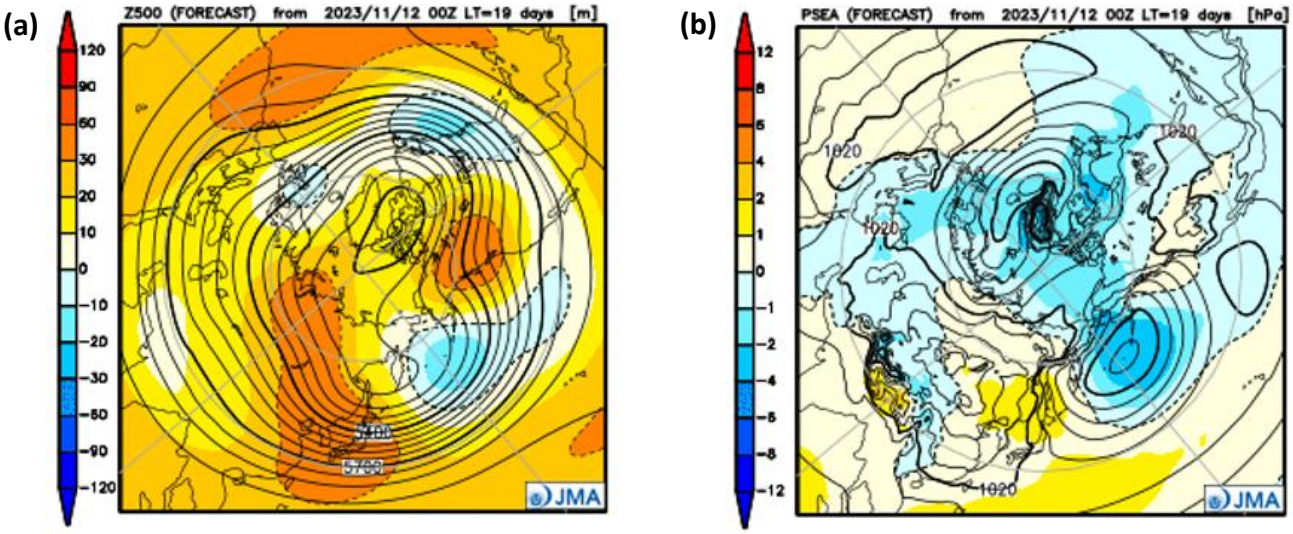

Figure 2-3 Predicted atmospheric fields over 20°N-90°N for December–February 2023/2024 (ensemble mean of 51 members)
(a) Geopotential height at 500-hPa (contours) and anomaly (shading). The contour interval is 60 m. (b) Sea level pressure (contours) and anomaly (shading). The contour interval is 4 hPa.

Note: JMA operates a seasonal Ensemble Prediction System (EPS) using the Coupled atmosphere-ocean General Circulation Model (CGCM) to make seasonal predictions beyond a one-month time range. The EPS produces perturbed initial conditions by means of a combination of the initial perturbation method and the lagged average forecasting (LAF) method. Prediction is made using 51 members from the latest 17 initial dates (3 members are used every day). Details of the prediction system and verification maps based on 30-year hindcast experiments (1991–2020) are available at https://www.data.jma.go.jp/tcc/tcc/products/model/.

(ITO Akira, Tokyo Climate Center)

<<Table of contents <Top of this article

Summary of the 2023 Asian Summer Monsoon

This report summarizes the characteristics of the surface climate and atmospheric/oceanographic considerations related to the Asian summer monsoon for 2023.

Note: The Japanese Reanalysis for Three Quarters of a Century (JRA-3Q) dataset (Kosaka et al. 2024) and MGDSST (Kurihara et al. 2006) were used to analyze atmospheric circulation and sea surface temperature (SST) in the research reported here. NOAA Climate Prediction Center (CPC) blended Outgoing Longwave Radiation (OLR) data from the NOAA website (https://ftp.cpc.ncep.noaa.gov/precip/CBO_V1/) were used to infer tropical convective activity. The base period for the normal is 1991 to 2020. The term “anomaly” as used in this report refers to deviation from the normal.

1. Precipitation and temperature

CLIMAT data on total precipitation for the monsoon season (June – September) showed more than 140% of the normal over Pakistan, northwestern India, northern Mongolia, parts of southeastern and northeastern China and southern Korea, while less than 60% of the normal was seen over southern Central Asia, in and around southern India, and in northern China and southern Indonesia (Figure 3-1 (a)). Notably, values exceeding 200% of the normal

were seen over Pakistan, and it was reported that heavy rain from June to August caused at least 1,380 fatalities from India to Afghanistan (sources: governments of India and Pakistan, EM-DAT). Monthly precipitation in India was the lowest on record for August since 1901 (India Meteorological Department).

Four-month mean temperatures for the same period were above normal in many parts of the area from Central Asia to East Asia, while values were below normal in and around Pakistan and over northwestern India (Figure 3-1 (b)). Monthly mean temperatures in Japan were at record highs since 1891 from May to September. The seasonal mean temperature in China from June to August was the second highest on record since 1961 (China Meteorological Administration). The monthly mean temperature in Korea was also the highest on record for September since 1973 (Korea Meteorological Administration). Intense heat is reported to have caused 94 fatalities in Japan (Fire and Disaster Management Agency of Japan, as of 29 September) and more than 50 in northeastern India in June (European Commission).

(a) (b)

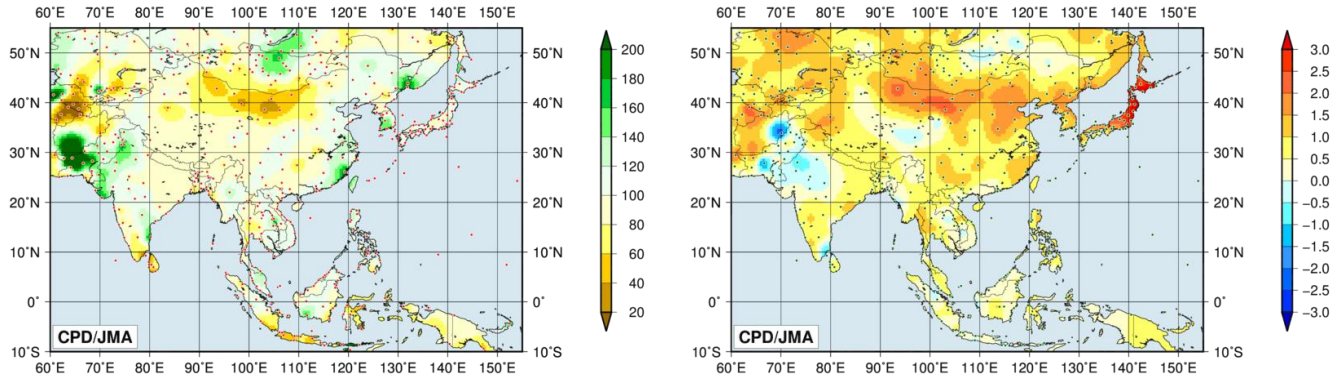

Figure 3-1 Four-month (a) precipitation ratios [%] and (b) mean temperature anomalies [°C] from June to September 2023
The base period for normal is 1991 – 2020. The red (a) and green (b) dots show stations providing map data, which are interpolated due to a lack of CLIMAT reporting and climatological normal values in some areas.

2. Tropical cyclones

There was a total of 14 named tropical cyclones (TCs) over the western North Pacific and the South China Sea by the end of September 2023, compared with the normal of 18.6 (Table 3-1). From June to September, there was a total of 12 named TCs (climatological normal: 16.1), with 11 approaches or landfalls on Southeast and East Asia and 8 (climatological normal: 9.5) on Japan. The series of TCs that formed over or around the Philippines in late July was associated with northward migration of enhanced convection from the equatorial western Pacific to the Philippines. This coincided with a phase-shift of intra-seasonal oscillation and intrusion of upper-level high-potential-vorticity (PV) air as described in Section 3.

Table 3-1 Named Tropical cyclones over the western North Pacific and the South China Sea by the end of September 2023

Name (number)		Date(UTC)	Category[1)]	Maximum wind[2)] (kt)
Sanvu	(2301)	20 Apr - 21 Apr	TS	45
Mawar	(2302)	20 May - 2 Jun	TY	115
Guchol	(2303)	6 Jun - 12 Jun	TY	80
Talim	(2304)	15 Jul - 18 Jul	STS	60
Doksuri	(2305)	21 Jul - 28 Jul	TY	100
Khanun	(2306)	28 Jul - 10 Aug	TY	95
Lan	(2307)	8 Aug - 17 Aug	TY	90
Dora	(2308)	12 Aug - 15 Aug	TY	80
Saola	(2309)	24 Aug - 2 Sep	TY	105
Damrey	(2310)	24 Aug - 29 Aug	STS	50
Haikui	(2311)	28 Aug - 4 Sep	TY	85
Kirogi	(2312)	30 Aug - 3 Sep	STS	50
Yun-yeung	(2313)	5 Sep - 8 Sep	TS	45
Koinu	(2314)	29 Sep - 9 Oct	TY	90

Note: Based on information from the RSMC Tokyo-Typhoon Center.
1) Intensity classification for tropical cyclones.
TS: tropical storm (34 – 47 kt), STS: severe tropical storm (48 – 63 kt), TY: typhoon (≥64 kt)
2) Estimated maximum 10-minute mean wind.
3) Based on early analysis data (rather than best track data) for tropical cyclones from Lan (2307) to Koinu (2314).
4) Dora (2308) entered the western North Pacific cross the International Date Line from the central North Pacific. The data are shown for the period when Dora existed over the western North Pacific.

3. Monsoon activity and atmospheric circulation

Convective activity inferred from OLR averaged for June – September 2023 (Figure 3-2) was enhanced from the equatorial Pacific to the seas east of the Philippines, while convective activity was suppressed from the central Indian Ocean to Southeast Asia. The anomalous convection observed from the central Indian Ocean to the equatorial Pacific is associated with a positive phase of the Indian Ocean Dipole (IOD) mode, which is characterized by negative SST anomalies in the southeastern tropical Indian Ocean, positive SST anomalies in the western tropical Indian Ocean, and the El Niño event (Figure 3-3). OLR index values (Table 3-2) indicate that the overall activity of the Asian summer monsoon (represented by the SAMOI (A) index) was below normal from May through August. The active convection area was shifted eastward of its normal position in the same period (see SAMOI (W) index).

Although the average activity of the Asian monsoon was weaker than normal during summer, convective activity in the Asian monsoon region exhibited remarkable intra-seasonal oscillation. Convection over India and the Bay of Bengal was suppressed in June and from late July to August, and was near normal from late June to mid-July (Figure 3-4 (a)). Convection over the Philippines showed variability with a period of approximately 30 – 60 days (Figure 3-4 (b)), possibly in association with boreal summer intra-seasonal oscillation (BSISO; Lee et al. 2013; Kikuchi 2021).

Convection variability also superimposes further variability with a quasi-biweekly period (Zhu et al. 2020, 2023). In July, enhanced convection migrated northwestward from the western equatorial Pacific to the Philippines, contributing to a series of TC occurrences and an intensified Pacific-Japan (PJ) pattern (Nitta 1987, Kosaka and Nakamura 2006) as presented later.

Figure 3-5 shows four-month mean 200- and 850-hPa stream function fields for June – September. In the upper troposphere (Figure 3-5 (a)), cyclonic circulation anomalies were seen over a wide area of Eurasia in association with suppressed convection from the central Indian Ocean to Southeast Asia, implying that extension of the Tibetan High was weaker than normal. The high was zonally split and remarkably deformed, with detached upper-level low PV air masses migrating toward northern Japan (Figure 3-6). Meanwhile, high PV air masses detached from the intensified mid-Pacific trough (Figure 3-5 (a)) and migrated toward the south of Japan (Figure 3-6), possibly contributing to enhanced convection and several related TC occurrences via dynamical ascent over areas south of Japan and east of the Philippines (Figure 3-2).

In the lower troposphere (Figure 3-5 (b)), anti-cyclonic circulation anomalies were seen from the Arabian Sea to the Bay of Bengal in association with suppressed convection from the central Indian Ocean to Southeast Asia (Figure 3-2). Meridional dipole anomalies along with cyclonic circulation anomalies from the area south of Japan to southeastern China and anti-cyclonic circulation anomalies to the east of Japan were seen in association with the intensified PJ pattern, contributing to intense heat in Japan from late July onward.

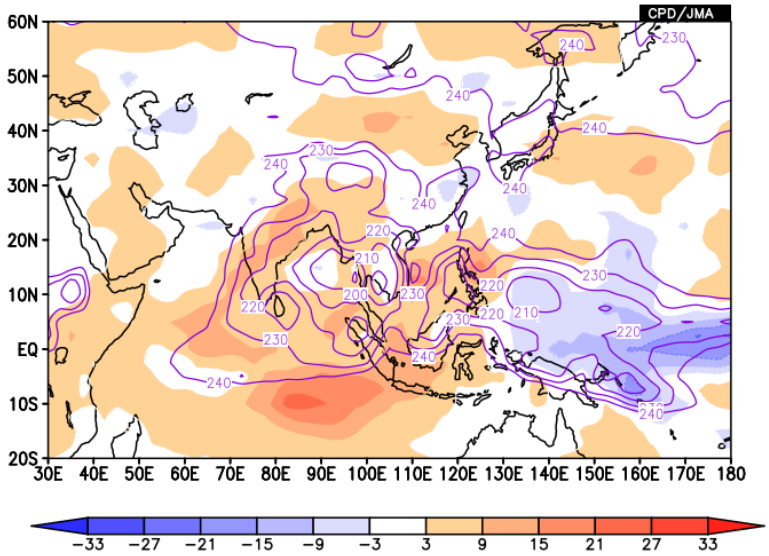

Figure 3-2 Four-month mean OLR [W/m²] for June–September 2023

Contours indicate OLR lower than 240 W/m² at intervals of 10 W/m², and color shading denotes OLR anomalies from the normal (i.e., the 1991–2020 average). Negative (cold color) and positive (warm color) OLR anomalies show enhanced and suppressed convection compared to the normal, respectively.

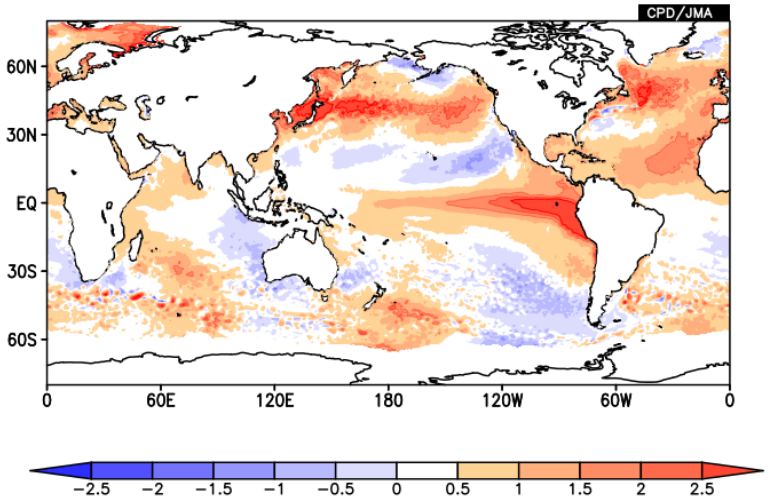

Figure 3-3 Four-month mean SST anomalies [°C] for June–September 2023
The base period for the normal is 1991 – 2020.

Table 3-2 Summer Asian Monsoon OLR Index (SAMOI) values observed from May to September 2023

Asian summer monsoon OLR indices (SAMOI) are derived from OLR anomalies. SAMOI (A), (N) and (W) indicate the overall activity of the Asian summer monsoon, its northward shift and its westward shift, respectively. SAMOI definitions are as follows: SAMOI (A) = (-1) × (W + E); SAMOI (N) = S – N; SAMOI (W) = E – W. W, E, N and S indicate area-averaged OLR anomalies for the respective regions shown in the figure on the right normalized by their standard deviations.

	Summer Asian Monsoon OLR Index (SAMOI)		
	SAMOI (A): Activity	SAMOI (N): Northward-shift	SAMOI (W): Westward-shift
May 2023	-1.0	-0.2	-1.8
Jun 2023	-1.3	-0.2	-1.3
Jul 2023	-0.6	-0.3	-1.6
Aug 2023	-3.2	+0.9	-0.7
Sep 2023	+0.4	-0.3	+1.4

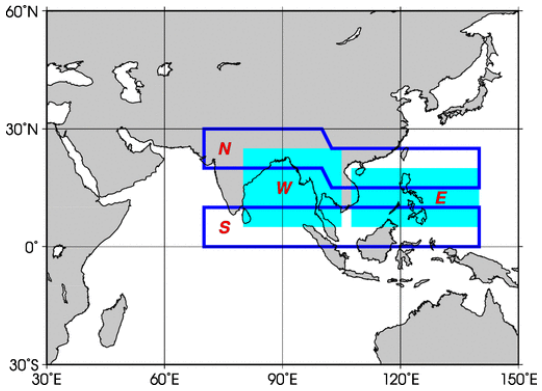

(a)

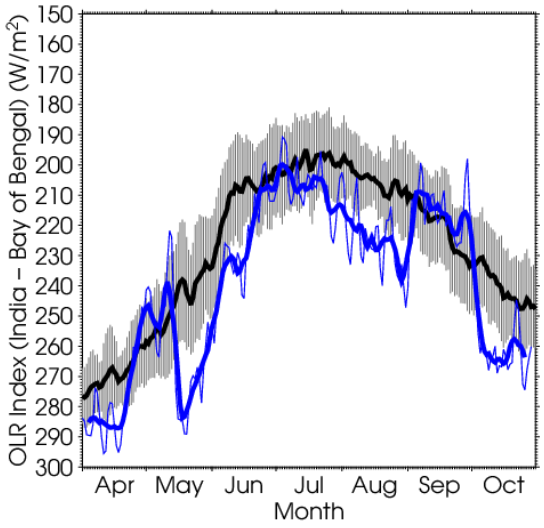

(b)

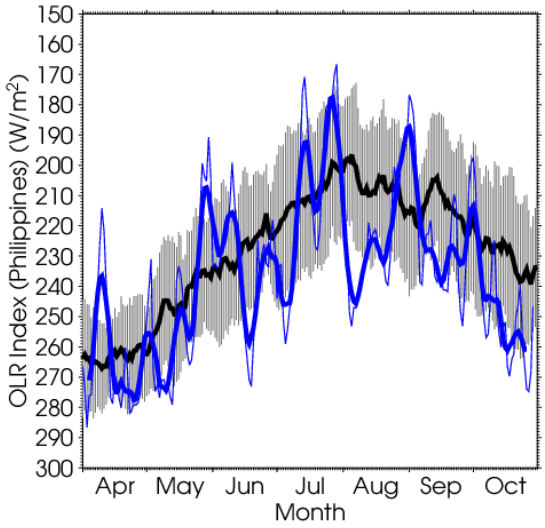

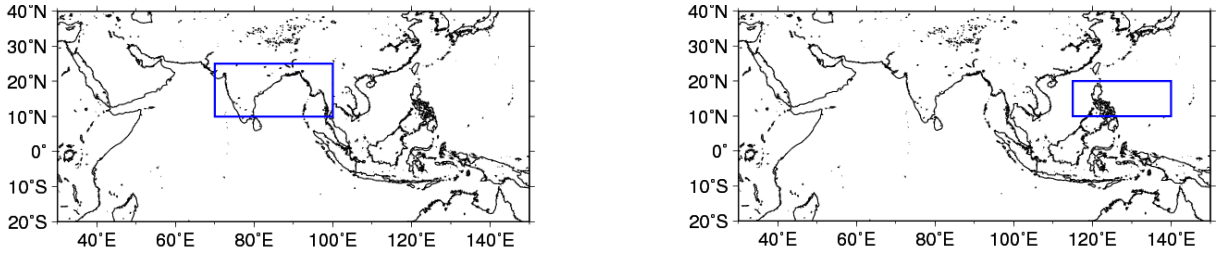

Figure 3-4 Time-series representation of OLR [W/m^2] averaged over (a) India and the Bay of Bengal (shown by the rectangle on the bottom: 10°N - 25°N, 70°E - 100°E) and (b) the Philippines (shown by the rectangle on the bottom: 10°N - 20°N, 115°E - 140°E)

The OLR indices are calculated after Wang and Fan (1999). The thick and thin blue lines indicate seven-day running mean and daily mean values, respectively. The black line denotes the normal (i.e., the 1991 - 2020 average), and the gray shading shows the range of the standard deviation calculated for the time period of the normal.

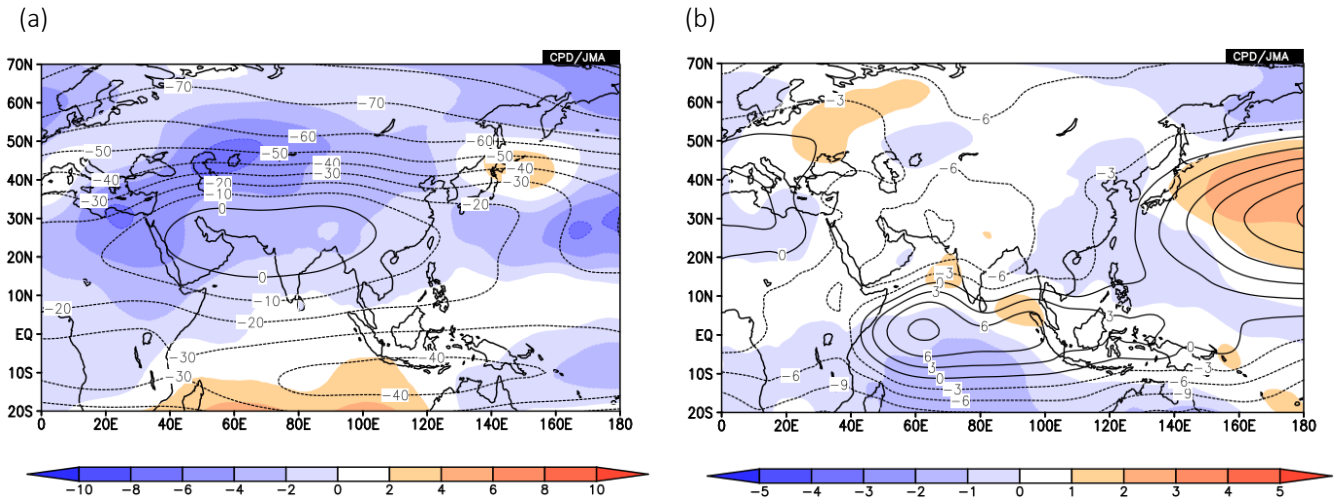

Figure 3-5 Four-month mean (a) 200-hPa and (b) 850-hPa stream function [10^6 m^2/s] for June–September 2023

Contours indicate stream function at intervals of (a) 10 × 10^6 m^2/s and (b) 3 × 10^6 m^2/s, and shading shows stream function anomalies. Red (blue) shading denotes anti-cyclonic (cyclonic) circulation anomalies in the Northern Hemisphere, and vice-versa in the Southern Hemisphere. The base period for the normal is 1991 – 2020.

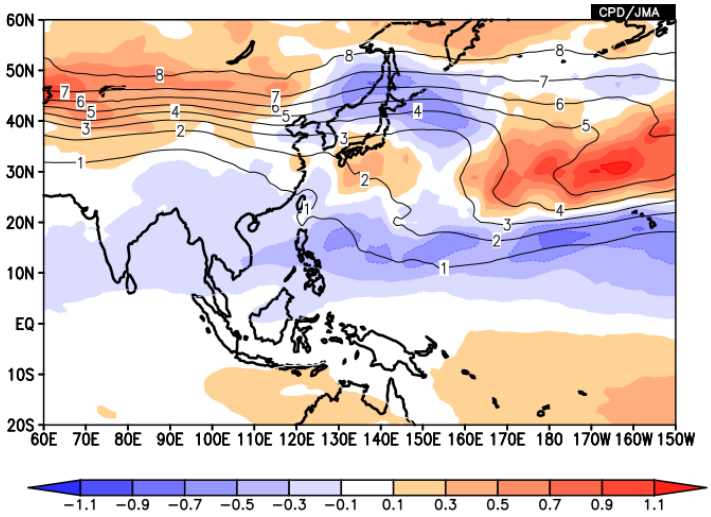

Figure 3-6 Four-month mean 360-K isentropic potential vorticity [PVU; 10^{-6}m^{2}s^{-1}K kg^{-1}] for June–September 2023

Shading indicates anomalies, and contours show potential vorticity at intervals of 1 PVU. The base period for the normal is 1991 – 2020.

References

Kikuchi, K., 2021: The boreal summer intraseasonal oscillation (BSISO): A review. *J. Meteor. Soc. Japan*, **99**, 933-972.

Kosaka Y., S. Kobayashi, Y. Harada, C. Kobayashi, H. Naoe, K. Yoshimoto, M. Harada, N. Goto, J. Chiba, K. Miyaoka, R. Sekiguchi, M. Deushi, H. Kamahori, T. Nakaegawa; T. Y. Tanaka, T. Tokuhiro, Y. Sato, Y. Matsushita, K. Onogi, 2024: The JRA-3Q Reanalysis. *J. Meteor. Soc. Japan*, **102**, Early Online Released.

Kosaka, Y., and H. Nakamura, 2006: Structure and dynamics of the summertime Pacific-Japan teleconnection pattern. *Quart. J. Roy. Meteor. Soc.*, **132**, 2009-2030.

Kurihara, Y., T. Sakurai, and T. Kuragano, 2006: Global daily sea surface temperature analysis using data from satellite microwave radiometer, satellite infrared radiometer and in-situ observations. *Weather Service Bulletin*, **73**, Special issue, s1-s18 (in Japanese).

Lee, J.-Y., B. Wang, M. C. Wheeler, X. Fu, D. E. Waliser, and I.-S. Kang, 2013: Real-time multivariate indices for the boreal summer intraseasonal oscillation over the Asian summer monsoon region. *Clim. Dyn.*, **40**, 493-509.

Nitta, T., 1987: Convective activities in the tropical western Pacific and their impact on the Northern Hemisphere summer circulation. *J. Meteor. Soc. Japan*, **65**, 373-390.

Wang, B. and Z. Fan, 1999: Choice of South Asian summer monsoon indices. *Bull. Amer. Meteor. Soc.*, **80**, 629–638.

Zhu, Y., Z. Wen, Y. Guo, R. Chen, X. Li, and Y. Qiao, 2020: The characteristics and possible growth mechanisms of the quasi-biweekly Pacific-Japan teleconnection in boreal summer. *Climate Dyn*., **55**, 3363-3380.

Zhu, Y., R. Chen, Q. Song, X. Li, Y. Guo, Z. Wen, 2023: An investigation of the maintenance mechanisms of the quasi-biweekly Pacific-Japan teleconnection. *Climate Dyn.*, https://doi.org/10.1007/s00382-023-06908-2.

(TAKEMURA Kazuto, Tokyo Climate Center)

<<Table of contents <Top of this article

Status of the Antarctic Ozone Hole in 2023

The annual maximum size of the Antarctic ozone hole in 2023 exceeded the most recent decadal average due to a large low-temperature area in the stratosphere.

Since the early 1980s, the Antarctic stratospheric ozone level has fallen every year in austral spring with a peak in September or early October. This area of depletion is referred to as the Antarctic ozone hole.

JMA analysis based on data from the Ozone Mapper Profiler Suite (OMPS) on board the Suomi National Polar-orbiting Partnership (NPP) satellite indicates that the 2023 Antarctic ozone hole appeared in early August and expanded rapidly from late August onward, exceeding the scale of the most recent decadal average (Figure 4-1, upper left). Its annual maximum size (observed on 21 September) was 25.9 million square kilometers (Figure 4-1, upper right), which is larger than the average over the most recent decade but slightly smaller than that observed in 2022 and around 1.9 times as large as Antarctica itself. In 2023 the polar vortex over Antarctica was stable until mid-September, and the low-temperature area in the stratosphere was larger than the most recent decadal average in September. These conditions had contributed to an expanded Antarctic ozone hole by mid-September due to

sustained formation of polar stratospheric clouds (PSCs), which play an important role in ozone depletion.

The *WMO/UNEP Scientific Assessment of Ozone Depletion: 2022* reports that total column ozone in the Antarctic continues to recover, notwithstanding substantial interannual variability in the size, strength and longevity of the ozone hole, and is expected to return to 1980 values around 2066.

The ozone layer acts as a shield against ultraviolet radiation, which can cause skin cancer. The Antarctic ozone hole was first recognized in the early 1980s, and large-scale events have been observed since the 1990s. Its maximum area on record was 29.8 million square kilometers (2000). Antarctic ozone depletion caused an expansion of the tropics and a poleward shift of the jet stream and storm tracks in the Southern Hemisphere that led to pronounced changes in summertime surface climate conditions according to recent assessment.

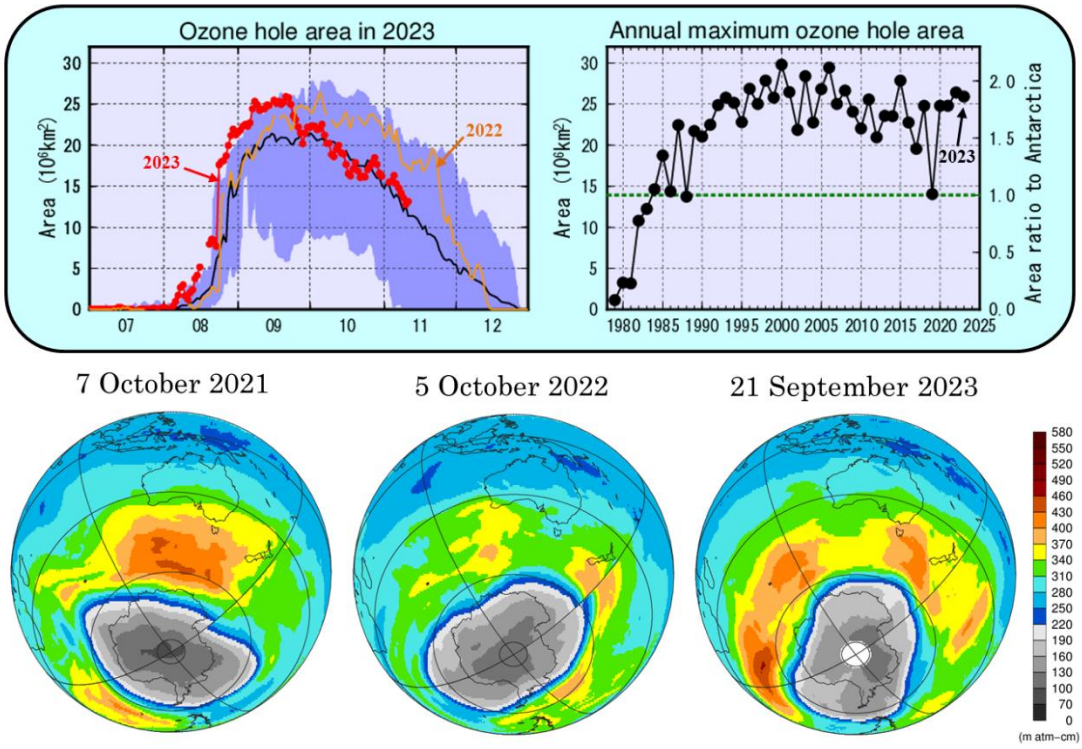

Figure 4-1 Antarctic ozone hole observation

Upper left: Time-series representation of the daily ozone hole area for 2023 (red line), 2022 (orange line) and the 2013 – 2022 average (black line). Blue shading represents the range of daily maxima and minima over the previous 10 years. JMA defines the extent of Antarctic ozone hole expansion area expanding as the area in which the total ozone column value is less than or equal to 220 m atm-cm.

Upper right: Inter-annual variability of the annual maximum ozone hole area. The green dotted line shows the area of the Antarctic Continent (13.9 million square kilometers).

Bottom: Snapshots of total column ozone distribution on the day of the annual maximum ozone hole area for the previous three years; the Antarctic ozone hole is shown in grey. Images are based on NASA satellite data.

(UEMURA Keiko, Atmospheric Environment and Ocean Division)

<<Table of contents <Top of this article

Status of the Arctic Sea Ice in 2023

It is virtually certain that there has been a long-term decreasing trend of sea ice extent in the Arctic Ocean since 1979, when the current method of monitoring using satellite sensors began. The trend is statistically significant at a confidence level of 99%. The reduction in the annual minimum extent is particularly notable at 0.086×10^6 km^2 per year up to 2023 (Figure 5-1).

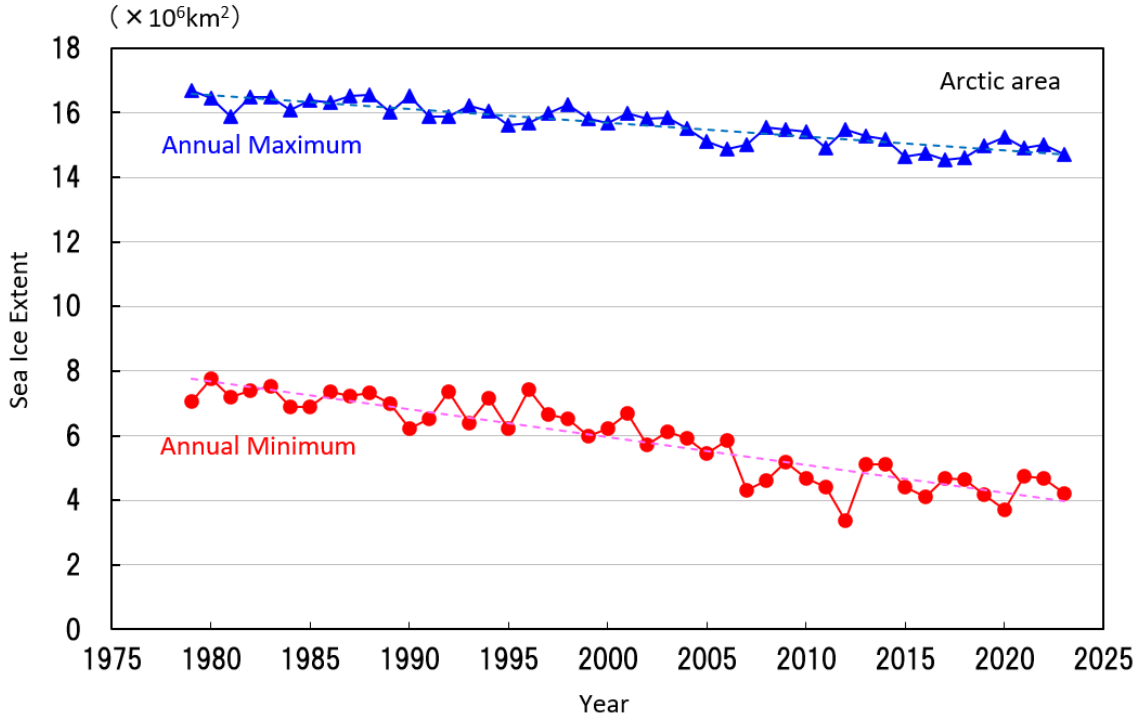

Figure 5-1Time-series representations of annual maximum and annual minimum sea ice extent in the Arctic Ocean (including the Sea of Okhotsk and the Bering Sea) from 1979 to 2023
Blue and red lines indicate annual maximum and annual minimum sea ice extents, respectively, with dashed lines indicating linear trends. Sea ice extents are calculated from brightness temperature data provided by NASA (the National Aeronautics and Space Administration) and NSIDC (the National Snow and Ice Data Center).

Based on preliminary analysis, the annual maximum Arctic sea ice extent was 14.72×10^6 km^2 on 2 March 2023, marking the 4th-lowest value since 1979. The value subsequently decreased during spring and summer in the Northern Hemisphere and reached its annual minimum of 4.21×10^6 km^2 on 16 September, marking the 5th-lowest level since 1979 (Figure 5-2, 5-3).

(HAMADA Keiji, Office of Marine Prediction)

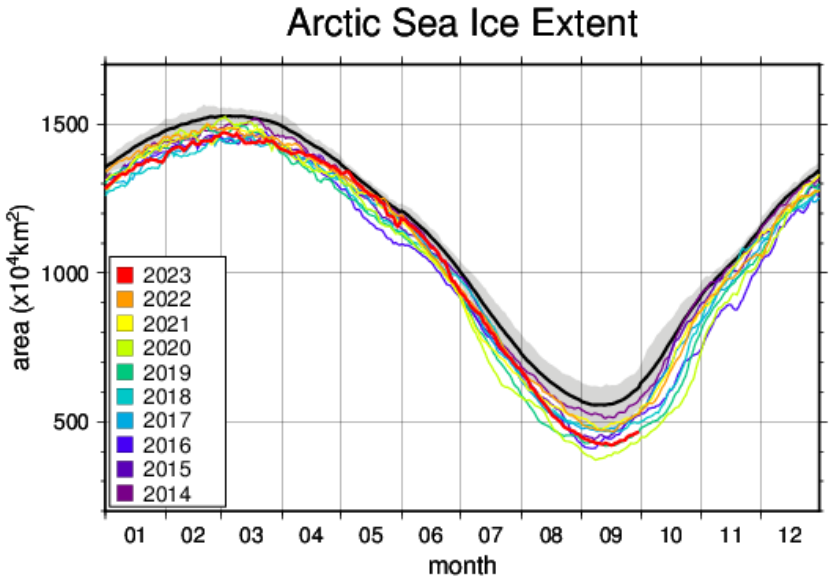

Figure 5-2 Annual variations in the Arctic sea ice extent
The black line represents the normal, and shading represents the normal range. The base period for the normal is 1991 – 2020.

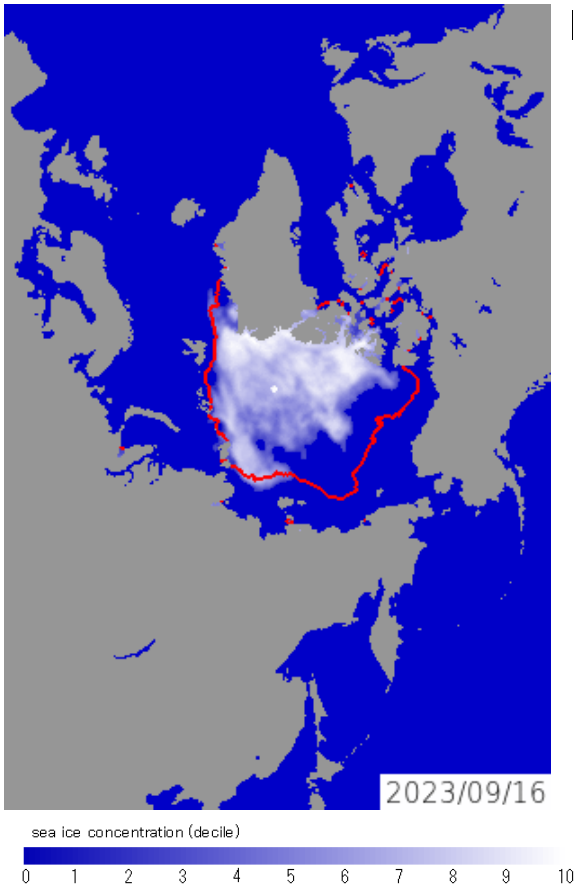

Figure 5-3 Annual minimum Arctic sea ice distribution
As of 16 September 2023. The red lines represent the normal extent. The base period for the normal is 1991 – 2020.

<<Table of contents <Top of this article

Eleventh session of the East Asia Winter Climate Outlook Forum

The World Meteorological Organization (WMO) actively supports the activities of the Regional Climate Outlook Forum (RCOF), which brings together experts from climatologically homogeneous regions and provides consensus-based seasonal predictions and information. As one of the RCOFs, the East Asia Winter Climate Outlook Forum (EASCOF) was jointly established by the China Meteorological Administration (CMA), the Japan Meteorological Agency (JMA), the Korea Meteorological Administration (KMA), and Mongolia's National Agency for Meteorology and Environment Monitoring (NAMEM) in 2012.

The eleventh session of EASCOF (EASCOF-11) was held at JMA's headquarters in Tokyo, Japan, from 6 to 8 November 2023 with a face-to face format for the first time in four years after restrictions related to COVID-19 were lifted. More than 30 experts from China, Japan, Mongolia and the Republic of Korea attended, sharing information on the status of and future plans for seasonal forecasting services in individual National Meteorological and Hydrological Services (NMHSs). The Forum also welcomed Dr. Wilfran Moufouma Okia as the first-ever direct attendee from WMO, which contributed highly to the interactions.

The attendees discussed recent understandings of phenomena related to the East Asian Winter Monsoon (EAWM) and seasonal outlooks for the coming winter. A very informative session on the latest forecast systems of individual NMHSs highlighted recent developments in each area, and another on good practices toward user involvement in climate services underlined the status of recent research activities from outside experts in the utilization of climate information.

The first session for Objective Seasonal Forecasts (OSF) as a follow-up to the RAII Operating Plan (OP) was led by Mr. Hirotaka Sato (JMA; Leader of the RAII Expert Team on Climate Services), with the Forum agreeing to continue discussions toward an optimal style of OSF for EASCOF.

The discussions held are expected to help develop attendees' understanding of phenomena related to EAWM and support improvement of their climate services. Forum materials are available on the EASCOF portal.

(TAKAHASHI Kiyotoshi, Tokyo Climate Center)

<<Table of contents <Top of this article

TCC and WMC Tokyo co-contributions to Regional Climate Outlook Forums

WMO Regional Climate Outlook Forums (RCOFs) bring together national, regional and international climate experts on an operational basis to produce regional climate outlooks based on input from participating NMHSs, regional institutions, Regional Climate Centres (RCCs) and global producers of climate predictions. By providing a platform for countries with similar climatological characteristics to discuss related matters, these forums ensure consistency in terms of access to and interpretation of climate information.

In autumn 2023, representatives from TCC and the World Meteorological Centre (WMC) Tokyo attended two online RCOFs. WMC Tokyo gave presentations about outlooks based on their model predictions.

- The 26th winter session of the South Asian Climate Outlook Forum (SASCOF-26), 26 – 27 September and 3 October
- The 21st session of the ASEAN Climate Outlook Forum (ASEANCOF-21), 17, 20 – 21 and 23 November

The WMC Tokyo representatives provided winter outlooks based on climate monitoring and forecast products from the TCC website, highlighting Copernicus Climate Change Service (C3S) multi-model ensemble prediction incorporating JMA's seasonal prediction system.

These activities are intended to support the output of country-scale outlooks by National Meteorological and Hydrological Services (NMHSs), and to contribute to the summarization of consensus outlooks as well as the reduction of climate disaster risk in the water, agriculture and health sectors for each target area. TCC and WMC Tokyo are committed to ongoing collaboration with operational climate communities to enhance progress in forecast skill and application of climate information toward the resolution of common issues and the realization of a world resilient to adverse climate conditions.

(NEMOTO Noboru and TAKAHASHI Kiyotoshi, Tokyo Climate Center)

<<Table of contents <Top of this article

You can also find the latest newsletter from Japan International Cooperation Agency (JICA).

JICA Magazine

https://jicamagazine.jica.go.jp/en/

"JICA Magazine" is a public relations magazine published by JICA. It introduces the current situation of developing countries around the world, the people who are active in the field, and the content of their activities.

Any comments or inquiry on this newsletter and/or the TCC website would be much appreciated.

Please e-mail to tcc@met.kishou.go.jp.

(Editors: NEMOTO Noboru, TAKAHASHI Kiyotoshi)

Tokyo Climate Center, Japan Meteorological Agency
3-6-9 Toranomon, Minato City, Tokyo 105-8431, Japan

TCC Website:
https://www.data.jma.go.jp/tcc/tcc/index.html

<Top of this article